Films of Bare Single-Walled Carbon Nanotubes from Superacids with Tailored Electronic and Photoluminescence Properties

Avishek Saha,[†,‡] Saunab Ghosh,[†,‡] R. Bruce Weisman,[†,‡] and Angel A. Martí[†,‡,⊥,*]

[†]Department of Chemistry, [⊥]Department of Bioengineering, and [‡]R. E. Smalley Institute for Nanoscale Science and Technology, Rice University, 6100 S. Main Street, Houston, Texas 77005, United States

ABSTRACT The use of single-walled carbon nanotubes (SWCNTs) in fabricating macroscopic devices requires addressing the challenges of nanotube individualization and organization in the desired functional architectures. Previous success in depositing bare SWCNTs from chlorosulfonic acid onto silicon oxide microporous and mesoporous nanoparticles has motivated this study of their deposition onto fused silica substrates. A facile dip-coating method is reported that produces thin homogeneous films in which the carbon nanotubes are not covered by surfactants or shortened by sonication. Photophysical, electrical, chemical, and morphological properties of these SWCNT films have been characterized. When prepared at low densities, the films exhibit near-IR photoluminescence from individualized SWCNTs, whereas when prepared at high densities the films behave as transparent conductors. Sheet resistance of 471 ohm/sq has been achieved with film transmittance of ~ 86%.

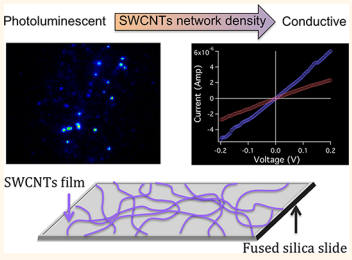

KEYWORDS: carbon nanotubes · conductive films · transparent films · photoluminescence · NIR microscopy

In the past few years, much research interest has been focused on the fabrication of random or oriented single-walled carbon nanotube (SWCNT) networks on various substrates. The motivation for forming such SWCNT films is their potential application in electronic devices such as organic light emitting displays,[1−3] thin film transistors,[4,5] and organic photovoltaics.[6,7] Conventional transparent conducting films of indium tin oxide (ITO) lack flexibility and have relatively high costs, whereas films based on SWCNTs could potentially display high flexibility and lower cost. Various film fabrication techniques have been reported, including spin coating,[8] spray coating,[9−12] bar coating,[13] dip coating,[14−18] drop casting,[19] and vacuum filtration.[20−24] All of these methods are classified as solution-based deposition techniques, as they require dispersing the SWCNTs in a suitable solvent, followed by deposition onto the substrate of interest. Spin coating is a simple and effective method for depositing SWCNTs on substrates, but it is not easily scaled up for large-scale fabrication. Spray coating is also a simple method, but it is not well suited to making uniform thin films because SWCNT droplets form an inhomogeneous distribution in the mist. Although vacuum filtration leads to uniform and reproducible films, the transfer process to suitable substrates may enhance the cost in industrial applications. Compared to all other aforementioned methods, dip coating is elegantly simple and has the advantage of scalability to large and nonplanar substrates.

In a previous publication we showed that SWCNTs protonated by chlorosulfonic acid (CSA) adhere efficiently to silicon oxide microporous and mesoporous particle surfaces.[25] We hypothesized that a similar behavior could be obtained for such protonated nanotubes (p-SWCNTs) on flat silicon oxide surfaces. Here we report the photophysical and electronic properties of films made by SWCNT deposition from CSA onto flat fused silica windows (Figure 1). Oddly, although fused silica is widely used in many applications including photovoltaics, monitors, LCD displays, and UV transparent windows, there seem to be no reports of two-dimensional SWCNT networks on fused silica. A detailed study of how to make such SWCNT films in fused silica, together with a thorough characterization of their properties, is pivotal for potential applications that range from display technologies to sensors to solar cells. In this report we

* Address correspondence to amarti@rice.edu.

Received for review May 11, 2012 and accepted June 1, 2012.

Published online June 08, 2012
10.1021/nn302092b

describe a general methodology to allow the straightforward fabrication of SWCNT films on fused silica substrates, with properties that can be tailored from highly photoluminescent to highly conductive by adjusting the nanotube concentration.

RESULTS AND DISCUSSION

Photoluminescence of Low-Density Thin Films. Individualization of SWCNTs was achieved by using CSA. CSA dissolves SWCNTs by reversibly protonating their walls, which results in Coulombic repulsion between CNTs and facilitates disaggregation by counteracting the strong intertube van der Waals attractions.[26,27] In a previous article, we reported that the *bulk* NIR-photoluminescence of p-SWCNTs can be regenerated by deprotonating the SWCNT surface.[25] To determine whether this process also occurs for CNTs deposited on fused silica, a film was made from a dilute SWCNT CSA solution and then treated with diethyl ether. Figure 2 shows the fluorescence image of such a film. Near-IR photoluminescence from isolated centers is observed, as is consistent with the presence of emissive individual SWCNTs. Further evidence that these spots correspond to SWCNTs comes from the variations in emission intensity of individual centers with excitation polarization (Figure 2b). The dominant absorption and emission transitions of SWCNTs are known to be strongly polarized parallel to the nanotube axis,[28,29] so the intensity modulation shown in Figure 2b is a signature of an individual SWCNT rather than an aggregate with randomly oriented nanotubes. We have also recorded spectra of the emissive centers that confirm their identities as individual SWCNTs. Figure 3 shows such spectra for seven different spots whose distinct peak positions indicate different (*n*,*m*) species. The peak wavelengths appear to be red-shifted from those reported for individual CVD-grown SWCNTs suspended in air, but they are similar to those observed for individual SWCNTs coated with surfactants. The emission full-widths at half-maximum, between *ca.* 15 and 23 meV, are also similar to those of surfactant-coated nanotubes[30,31] and broader than spectral widths reported for SWCNTs in air.[32−34] As these samples had not been exposed to surfactants, we suggest that the spectral differences compared to air-suspended SWCNTs arise from interactions with the fused silica substrate.

We also noted significant loss of SWCNT photoluminescence after the films on fused silica had been exposed to air for several days. This exciton quenching effect seems consistent with the reversible surface oxidation of SWCNTs reported by Dukovic *et al.*[35] Following this slow reduction of emission, the photoluminescence efficiency of our films could be restored by an additional immersion in diethyl ether. We suggest that p-doping caused by atmospheric oxygen in the presence of residual acid is reversed by proton transfer to diethyl ether, through a reaction analogous to the acid-catalyzed ether fission that is well known in organic chemistry.[36]

Decreased photoluminescence efficiency was also observed for films prepared from more concentrated SWCNT solutions. We attribute this effect to electronic coupling between contacted nanotubes. Such coupling allows optical excitation energy to flow from semiconducting to metallic SWCNTs, where rapid nonradiative decay prevents luminescence. We note that fluorescence was still observable from individual SWCNTs in films prepared from nanotube concentrations as

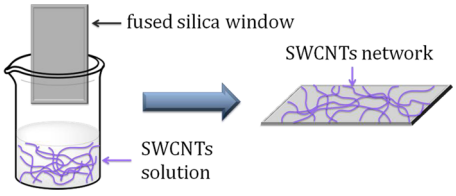

Figure 1. Pictorial representation of the deposition of SWCNTs onto a fused silica surface from CSA by dip coating.

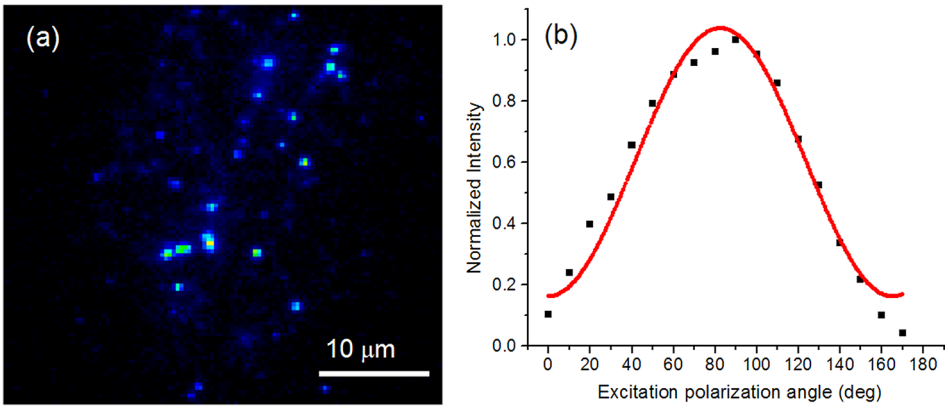

Figure 2. (a) Near-IR fluorescence image of SWCNTs on a fused silica slide prepared by deposition from a 5 μg/mL solution in CSA followed by deprotonation with diethyl ether. (b) Normalized intensity of an individual emission spot *vs* excitation beam polarization angle. The solid curve is a fit of the form $\sin^2\theta$.

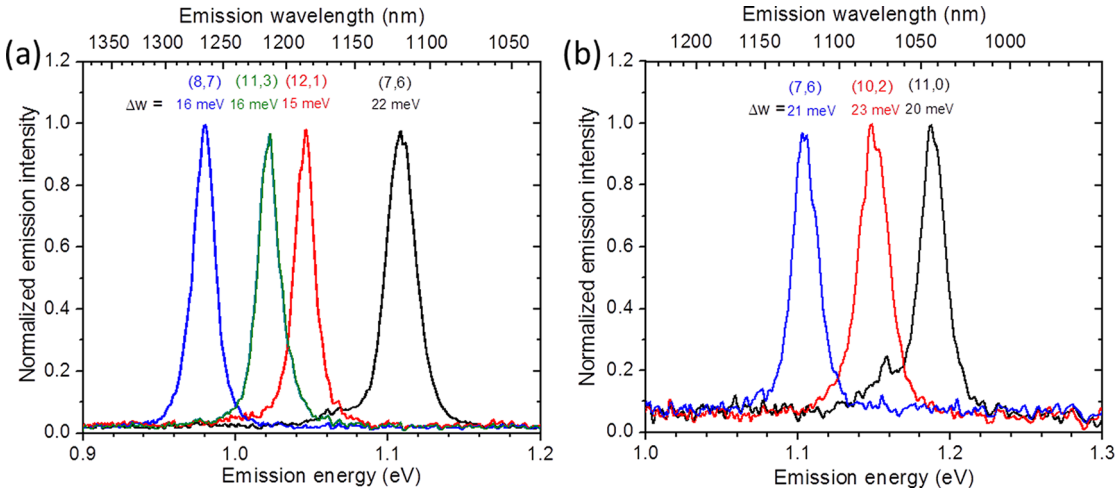

Figure 3. Normalized emission spectra of individual tubes dried on fused silica substrate upon (a) 785 nm and (b) 840 nm laser excitation.

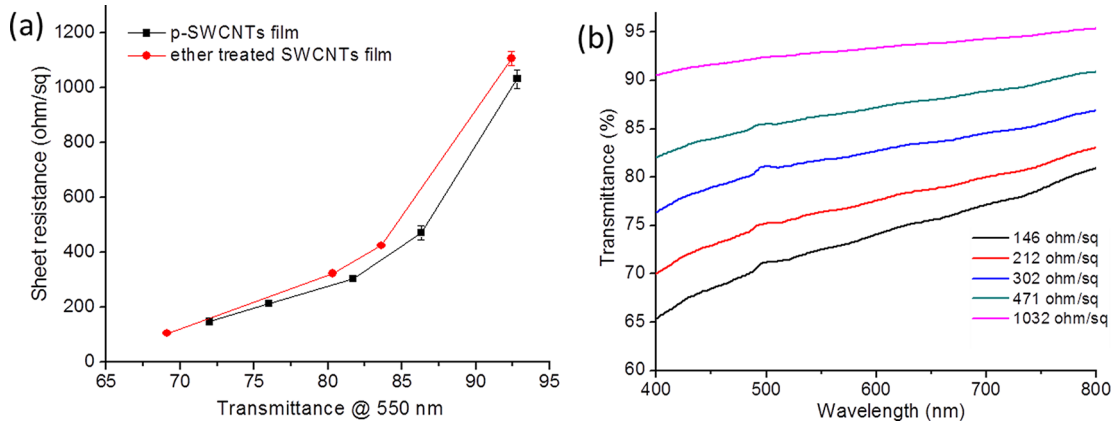

Figure 4. (a) Sheet resistance *vs* transmittance of SWCNTs films with different transparencies. In one series, sheet resistance of p-SWCNTs films was measured after fabrication. Other separate deprotonated films were produced by treating the films with diethyl ether before taking sheet resistance measurements. (b) Transmittance of p-SWCNTs films with different sheet resistances at visible wavelengths.

high as 0.03 mg/mL in CSA. (See Supporting Information, Figure S1.)

Transparent Conductive Films. Our studies indicate that the decreased SWCNT photoluminescence in denser nanotube networks is accompanied by an increase in conductivity of the film. To prepare conductive films, it is desirable to have a closely packed interconnected network of SWCNTs to increase the number of electrical pathways. We hypothesized that p-SWCNTs would have high affinities toward nonporous flat fused silica substrates, similar to those of mesoporous aluminosilicates in spite of the morphological differences. By varying the dipping time and concentration of the SWCNT solutions, we obtained CNT networks with different densities, allowing study of their optical and conductive properties. A common way to show the performance of conductive thin films is by plotting sheet resistance *vs* transmittance of visible light (usually at 550 nm, near the peak of the eye's response curve). As the film transparency decreases in denser networks of SWCNTs, the number of electrical pathways increases, reducing the sheet resistance. Resistive touch-screen applications require films with high visible transparency and low sheet resistance (85−90% transmittance and 300−500 ohm/sq sheet resistance).[9,37] Figure 4 shows our results for sheet resistance *vs* transmittance (along with visible transmission spectra) for different SWCNT depositions. We achieved sheet resistance as low as 212 and 471 ohm/sq with transmittance of ~76% and ~86%, respectively, which slightly outperforms films made of metallic sorted HiPco SWCNTs (*ca.* 231 ohm/sq with 75% transmittance).[22] It is notable that we find similar performance (Figure 4a) for films made from p-SWCNTs and p-SWCNTs after ether-treated (which are deprotonated), despite previous reports that acid-doped SWCNTs should give higher film conductivities.[38] The reasons for this lack of doping enhancement are not yet clear, but it seems possible that the identity of the conjugate base and the degree of protonation play roles in modulating

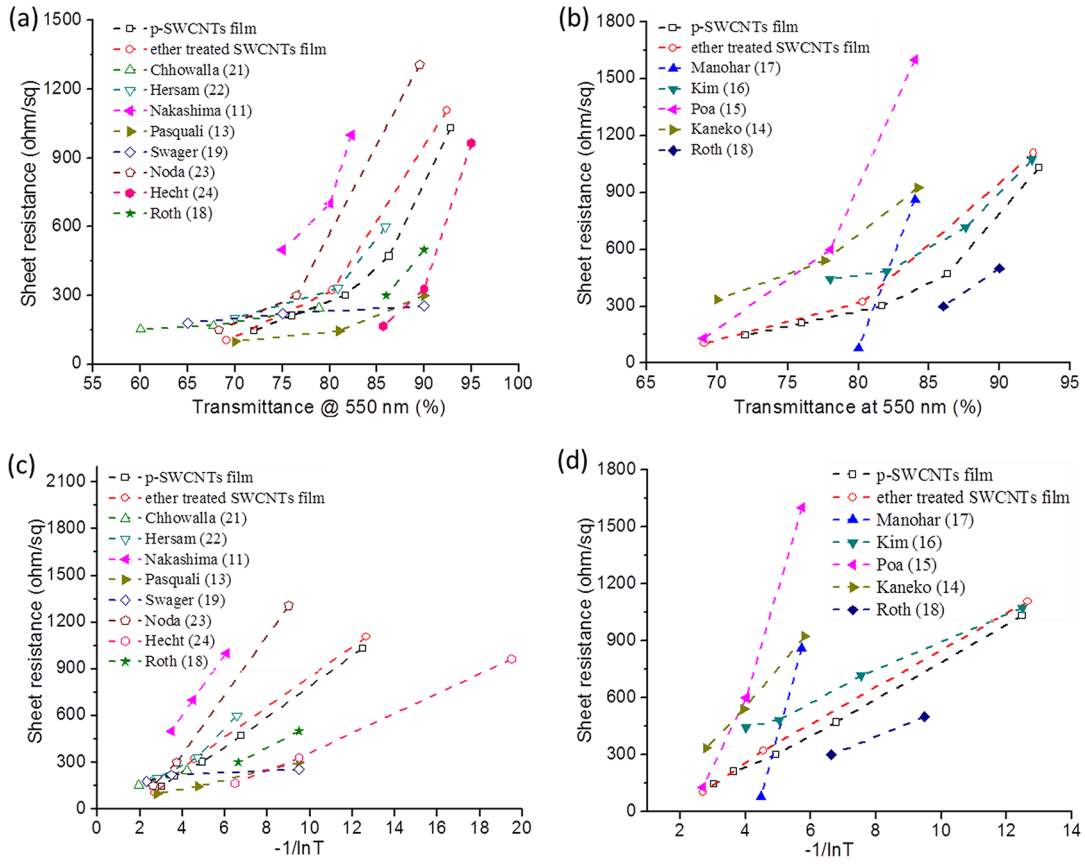

Figure 5. Performance comparison of our p-SWCNTs and ether-treated films with previously reported (a) HiPco films and (b) dip-coated films. Parts (c) and (d) show comparative FOM plots for HiPco and dip coating, respectively.

the conductivity of the films. Evidence of doping in p-SWCNT film is evident from X-ray photoelectron spectra (see below).

The performance of transparent conductive films can also be expressed with a figure of merit (FOM), which can be described in different but essentially equivalent ways. Recently Dan *et al.* formulated the following relation between sheet resistance (R_s) and transmittance (T):[13]

$$R_s = -\frac{\alpha\rho}{\ln T} \quad (1)$$

Here the product of the Beer–Lambert absorption coefficient (α) and resistivity (ρ) was defined as the FOM. The advantage of using ($\alpha\rho$) as a FOM is that it is independent of the film thickness. It is known that the properties of conductive SWCNT films depend strongly on the type of nanotubes they contain and on the fabrication method.[18,23,39] We therefore chose to compare the performance of our films with others that were made from HiPco SWCNTs or were prepared using dip coating. Figure 5a and b show previously reported sheet resistance *vs* transmittance data for these two classes of conductive SWCNT films, along with our current findings. It can be seen that our p-SWCNT and ether-treated films show performance comparable with some of the best prior reports. We note that almost all of the other films included in this comparison had been further doped with either HNO_3 or $SOCl_2$ before sheet resistance measurements. Figure 5c and d show FOM plots, based on eq 1, for HiPco and dip-coated films. In these figures, sheet resistance varies linearly with $-1/\ln T$, with a slope equal to FOM ($\alpha\rho$). Thus, films with favorable properties (higher transparency and lower sheet resistance) will show lower slopes (lower FOM) in Figure 5c and d. Roth and co-workers have reported HiPco dip-coated conductive films with slightly better FOM than the ones prepared in this study.[18] Interestingly, they suspended the CNTs in surfactants using strong sonication, which would lead to SWCNTs significantly shorter than the ones we used.[40] The fact that such networks of shorter SWCNTs showed better performance than the networks of long, bare SWCNTs used here challenges the current understanding of SWCNT film conductivity, such as the finding of Hecht *et al.* that electrical conductivity increases as average bundle length raised to the power 1.46.[41] There is clearly a need for further fundamental studies to clarify the factors that control electrical properties in CNT two-dimensional networks.

When we measured sheet resistance at various positions to study the spatial uniformity of our SWCNT films on fused silica, we observed that resistance

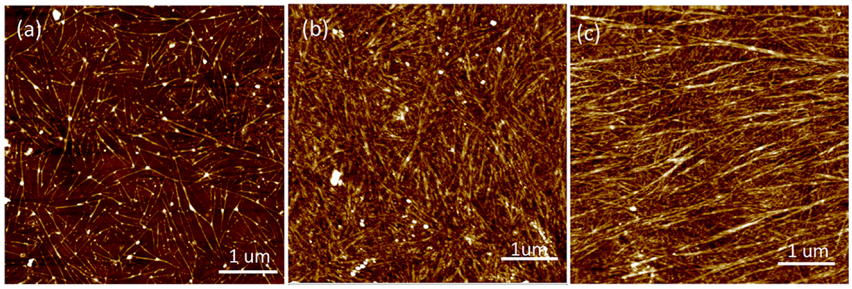

Figure 6. AFM images of SWCNT films prepared from SWCNT solutions of (a) 0.05 mg/mL, (b) 1 mg/mL (~90% transparency), and (c) 2 mg/mL (~70% transparency) concentrations.

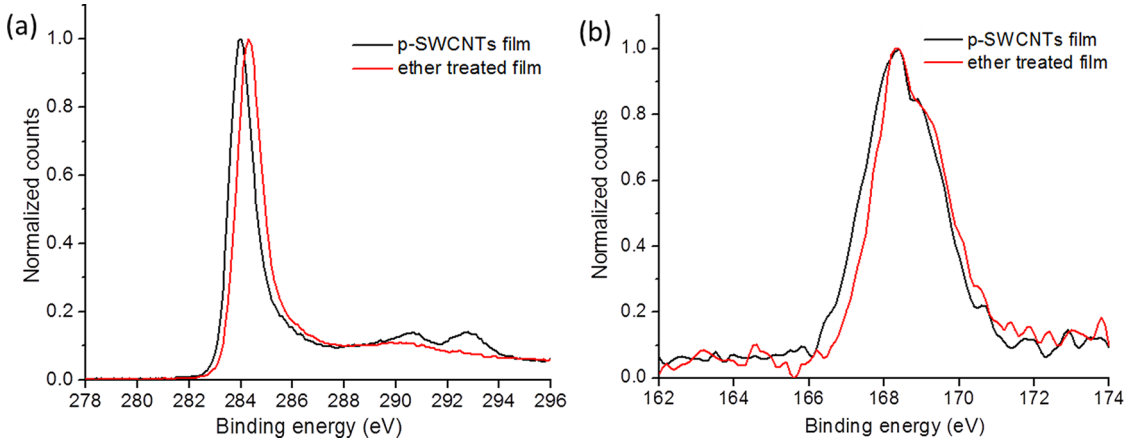

Figure 7. High-resolution XPS spectra of thin SWCNT films on fused silica substrate in the (a) C1s region and (b) S2p region.

variations decreased with increasing initial concentration of SWCNTs in CSA. This observation may reflect the formation of more homogeneous SWCNT networks at higher concentrations, giving a more uniform sheet resistance.

Structural Characterization of Films. Figure 6 shows atomic force microscopy (AFM) images of SWCNT thin films coated on fused silica using different concentrations of SWCNTs in CSA. As can be seen from the figure, CNTs form a continuous web over the substrate, where larger bundles of SWCNTs become more prevalent as the concentration is increased, and preferential orientation of these bundles becomes noticeable.

X-ray photoelectron spectroscopy (XPS) was used to investigate the chemical modification of the dry nanotube films before and after quenching with diethyl ether (see Figure 7). The large C1s peak due to sp^2-hybridized carbon appears at 284.0 and 284.3 eV for p-SWCNT and ether-quenched films, respectively. The downshift of p-SWCNTs is consistent with p-type doping.[42] For the p-SWCNTs films, we observe small shoulder peaks in the higher energy range of 290–293 eV. These unexpected shoulder peaks are likely due to the presence of $-CF_2$ moieties.[43] Arguably, mild oxidation of nanotube sidewalls might also be responsible for the presence of the small peaks. However the presence of fluorine in the survey spectra (see Supporting Information, Figure S2) supports the assignment to $-CF_2$ groups, which could represent contamination from the PTFE septa used for our preparations. These shoulder peaks essentially disappeared on treatment with diethyl ether. The weak signal near 168 eV in the S2p region probably comes from residual SO_3Cl. Sreekumar *et al.* also observed the S2p XPS spectra in their SWCNT films prepared from oleum dispersions.[44] However, we did not observe any additional S2p peak at 164.1 eV, which indicates the absence of any S in the (II) oxidation state (–C–S–C– bond).[23,42] Our XPS results show that carbon atoms are not significantly oxidized or chemically bonded to sulfur during film preparation.

The Raman spectra of diethyl ether-treated nanotube films excited at 785 nm are presented in Figure 8. The peak intensity ratio between the D band (disorder mode near 1300 cm^{-1}) and G band (tangential mode at *ca.* 1590 cm^{-1}) is ~1/7, ~1/8, and ~1/16 for the films with 92.4%, 80.3%, and 69.1% transparencies, respectively. These ratios are larger than for pristine HiPco samples (less than 1/20). The increased D/G ratio suggests sidewall defect formation, which may have been catalyzed by the fused silica surface during the heating step used to remove excess solvent. The lower D/G ratio in higher density films could then be attributed to thicker films that have a significant population of CNTs shielded from direct contact with the fused silica surface (see Figure 6). For Raman spectra of HiPco samples measured with 785 nm excitation, the

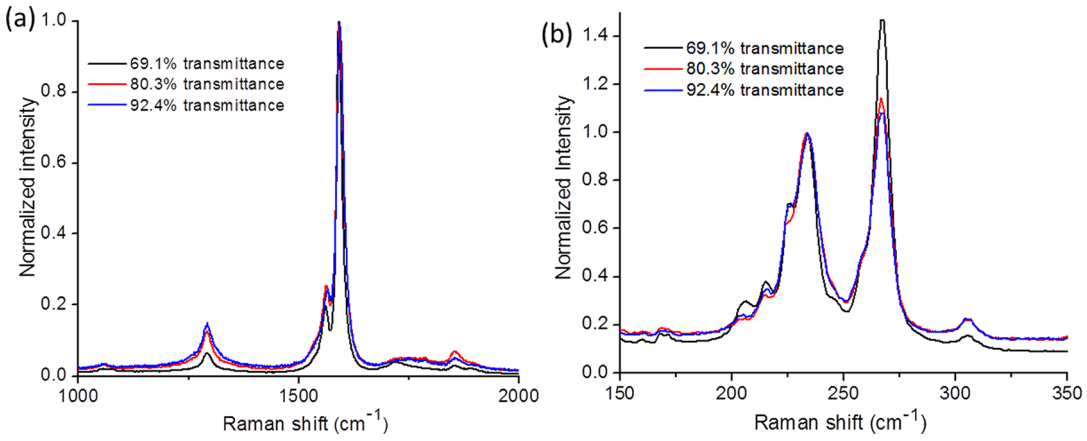

Figure 8. (a) Raman spectra of the SWCNT films of three different transparencies after quenching with diethyl ether; peaks are normalized with respect to the G-band intensity. (b) Radial breathing mode region of SWCNT films of three different transparencies; peaks are normalized with respect to 233 cm^{-1} peak intensity.

radial breathing mode (RBM) feature at 267 cm^{-1} is associated with bundled SWCNTs.[45,46] Figure 7b shows an increase in the relative intensity of this peak as the film transparency decreases from 92.4% to 69.1%, indicating an increased proportion of bundled nanotubes in the thicker films. Still, judging from the RBM intensities, the degree of aggregation is nonetheless lower than in as-produced undispersed pristine SWCNTs.

CONCLUSIONS

In summary, we report a simple and easily scalable technique that allows the preparation of SWCNT thin films with tailored properties. Fused silica substrates are dip coated in solutions of SWCNTs in chlorosulfonic acid. Adjusting the concentration of this solution allows the preparation of low-density SWCNT networks showing strong photoluminescence or higher density networks that form transparent conductive films. A clear advantage of this methodology is that "bare" SWCNTs free of surfactant coatings are quickly deposited on the fused silica surface, and the SWCNTs are not shortened by ultrasonic processing prior to deposition, as is generally the case in surfactant-based methods. The performance of these films as transparent conductors is competitive with state-of-the-art nanotube-based films recently reported by other groups. We expect that our solution-based dip-coating process will enable low-cost and large-scale production of thin films with conductive or photoluminescent properties.

EXPERIMENTAL SECTION

Materials. The SWCNTs used in this study were synthesized by the high-pressure carbon monoxide (HiPco) process at Rice University and were purified by low-temperature oxidative annealing and acid treatment as reported elsewhere.[47] Planar fused silica windows (12.5 × 45 mm) were obtained from Starna Cells. ACS certified chlorosulfonic acid (density = 1753 kg/m^3) was used as received from Sigma Aldrich.

SWCNT Film Preparation. Concentrated solutions of SWCNTs in CSA (1.0 mg/mL, 1.5 mg/mL and 2.0 mg/mL) were prepared following reported procedures.[25] Fused silica slides were thoroughly cleaned with chromic acid (to remove impurities), dried at 450 °C, and immersed vertically (manually) in a beaker containing a SWCNT solution of the desired concentration for 0 to 20 s. The dipping procedures were carried out in a glovebox with a constant dry air supply to keep the humidity to a minimum. Then the substrates were dried at 150 °C under vacuum for 20 min. Four-probe measurements were performed after drying the film to determine its resistance. Since dip coating covered both sides of the fused silica window, one side was wiped off thoroughly before making the transmittance measurements. Deprotonated SWCNT films were produced by immersion in diethyl ether for 60 s. The deprotonated SWCNT films were then dried under vacuum for about 10 min before measuring the sheet resistance. For near-IR photoluminescence experiments, fused silica windows were dipped into SWCNT-CSA solutions with concentrations ranging from 0.005 to 1 mg/mL. These films were typically dried at ca. 100 °C for about 10 min or directly dipped in ether for *ca.* 5 min.

Characterization. Fluorescence microscopy of individual semiconducting SWCNTs (on fused silica substrates) was performed using a customized Nikon TE-2000U inverted microscope equipped with a Nikon Plan 60× (NA = 1) water immersion objective and an InGaAs camera.[30] SWCNT fluorescence was excited with light from a CW Ti:sapphire laser at 785 or 840 nm. We measured the optical transmission of dense nanotube films at 550 nm using a UV–vis spectrophotometer (Shimadzu UV-2450). The sheet resistances of SWCNT films on fused silica were determined with a Keithley 2400 sourcemeter and a linear four-point probe. Raman spectra were obtained using a Renishaw inVia MicroRaman spectrometer. We measured X-ray photoelectron spectra on a PHI Quantera SXM scanning X-ray microprobe.

Conflict of Interest: The authors declare no competing financial interest.

Acknowledgment. This research was supported by grants from the National Science Foundation (CHE-1112374 to R.B.W. and CHE-1007483 to A.A.M.) and the Welch Foundation (C-0807 to R.B.W. and C-1743 to A.A.M.).

Supporting Information Available: Near-IR fluorescence image of SWCNTs deposited on fused silica from a 0.03 mg/mL CSA solution, and survey XPS spectra of p-SWCNTs and ether-treated films. This material is available free of charge *via* the Internet at http://pubs.acs.org.

REFERENCES AND NOTES

1. Li, J.; Hu, L.; Wang, L.; Zhou, Y.; Grüner, G.; Marks, T. J. Organic Light-Emitting Diodes Having Carbon Nanotube Anodes. *Nano Lett.* **2006**, *6*, 2472–2477.
2. Ou, E. C. W.; Hu, L.; Raymond, G. C. R.; Soo, O. K.; Pan, J.; Zheng, Z.; Park, Y.; Hecht, D.; Irvin, G.; Drzaic, P.; *et al.* Surface-Modified Nanotube Anodes for High Performance Organic Light-Emitting Diode. *ACS Nano* **2009**, *3*, 2258–2264.
3. Zhang, D. H.; Ryu, K.; Liu, X. L.; Polikarpov, E.; Ly, J.; Tompson, M. E.; Zhou, C. W. Transparent, Conductive, and Flexible Carbon Nanotube Films and their Application in Organic Light-Emitting Diodes. *Nano Lett.* **2006**, *6*, 1880–1886.
4. Bradley, K.; Gabriel, J.-C. P.; Grüner, G. Flexible Nanotube Electronics. *Nano Lett.* **2003**, *3*, 1353–1355.
5. Artukovic, E.; Kaempgen, M.; Hecht, D. S.; Roth, S.; Grüner, G. Transparent and Flexible Carbon Nanotube Transistors. *Nano Lett.* **2005**, *5*, 757–760.
6. Bernardi, M.; Giulianini, M.; Grossman, J. C. Self-Assembly and its Impact on Interfacial Charge Transfer in Carbon Nanotube/P3HT Solar Cells. *ACS Nano* **2010**, *4*, 6599–6606.
7. van de Lagemaat, J.; Barnes, T. M.; Rumbles, G.; Shaheen, S. E.; Coutts, T. J.; Weeks, C.; Levitsky, I.; Peltola, J.; Glatkowski, P. Organic Solar Cells with Carbon Nanotubes Replacing In_2O_3: Sn as the Transparent Electrode. *Appl. Phys. Lett.* **2006**, *88*, 233503.
8. Jo, J. W.; Jung, J. W.; Lee, J. U.; Jo, W. H. Fabrication of Highly Conductive and Transparent Thin Films from Single-Walled Carbon Nanotubes Using a New Non-ionic Surfactant *via* Spin Coating. *ACS Nano* **2010**, *4*, 5382–5388.
9. Geng, H. Z.; Kim, K. K.; So, K. P.; Lee, Y. S.; Chang, Y.; Lee, Y. H. Effect of Acid Treatment on Carbon Nanotube-Based Flexible Transparent Conducting Films. *J. Am. Chem. Soc.* **2007**, *129*, 7758–7759.
10. Tenent, R. C.; Barnes, T. M.; Bergeson, J. D.; Ferguson, A. J.; To, B.; Gedvilas, L. M.; Heben, M. J.; Blackburn, J. L. Ultrasmooth, Large-Area, High-Uniformity, Conductive Transparent Single-Walled-Carbon-Nanotube Films for Photovoltaics Produced by Ultrasonic Spraying. *Adv. Mater.* **2009**, *21*, 3210–3216.
11. Liu, Q. F.; Fujigaya, T.; Cheng, H. M.; Nakashima, N. Free-Standing Highly Conductive Transparent Ultrathin Single-Walled Carbon Nanotube Films. *J. Am. Chem. Soc.* **2010**, *132*, 16581–16586.
12. Paul, S.; Kang, Y. S.; Yim, J. H.; Cho, K. Y.; Kim, D. W. Effect of Surfactant and Coating Method on the Electrical and Optical Properties of Thin Conductive Films Prepared with Single-Walled Carbon Nanotubes. *Curr. Appl. Phys.* **2010**, *10*, E101–E104.
13. Dan, B.; Irvin, G. C.; Pasquali, M. Continuous and Scalable Fabrication of Transparent Conducting Carbon Nanotube Films. *ACS Nano* **2009**, *3*, 835–843.
14. Song, Y. I.; Yang, C. M.; Kim, D. Y.; Kanoh, H.; Kaneko, K. Flexible Transparent Conducting Single-Wall Carbon Nanotube Film with Network Bridging Method. *J. Colloid Interface Sci.* **2008**, *318*, 365–371.
15. Ng, M. H. A.; Hartadi, L. T.; Tan, H.; Poa, C. H. P. Efficient Coating of Transparent and Conductive Carbon Nanotube Thin Films on Plastic Substrates. *Nanotechnology* **2008**, *19*, 205703.
16. Jang, E. Y.; Kang, T. J.; Im, H. W.; Kim, D. W.; Kim, Y. H. Single-Walled Carbon-Nanotube Networks on Large-Area Glass Substrate by the Dip-Coating Method. *Small* **2008**, *4*, 2255–2261.
17. Saran, N.; Parikh, K.; Suh, D. S.; Munoz, E.; Kolla, H.; Manohar, S. K. Fabrication and Characterization of Thin Films of Single-Walled Carbon Nanotube Bundles on Flexible Plastic Substrates. *J. Am. Chem. Soc.* **2004**, *126*, 4462–4463.
18. de Andrade, M. J.; Lima, M. D.; Skakalova, V.; Bergmann, C. P.; Roth, S. Electrical Properties of Transparent Carbon Nanotube Networks Prepared through Different Techniques. *Phys. Status Solidi-Rapid Res. Lett.* **2007**, *1*, 178–180.
19. Gu, H.; Swager, T. M. Fabrication of Free-standing, Conductive, and Transparent Carbon Nanotube Films. *Adv. Mater.* **2008**, *20*, 4433–4437.
20. Wu, Z.; Chen, Z.; Du, X.; Logan, J. M.; Sippel, J.; Nikolou, M.; Kamaras, K.; Reynolds, J. R.; Tanner, D. B.; Hebard, A. F.; *et al.* Transparent, Conductive Carbon Nanotube Films. *Science* **2004**, *305*, 1273–1276.
21. Parekh, B. B.; Fanchini, G.; Eda, G.; Chhowalla, M. Improved Conductivity of Transparent Single-Wall Carbon Nanotube Thin Films *via* Stable Postdeposition Functionalization. *Appl. Phys. Lett.* **2007**, *90*, 121913.
22. Green, A. A.; Hersam, M. C. Colored Semitransparent Conductive Coatings Consisting of Monodisperse Metallic Single-Walled Carbon Nanotubes. *Nano Lett.* **2008**, *8*, 1417–1422.
23. Wang, Y.; Di, C.-A.; Liu, Y.; Kajiura, H.; Ye, S.; Cao, L.; Wei, D.; Zhang, H.; Li, Y.; Noda, K. Optimizing Single-Walled Carbon Nanotube Films for Applications in Electroluminescent Devices. *Adv. Mater.* **2008**, *20*, 4442–4449.
24. Hecht, D. S.; Heintz, A. M.; Lee, R.; Hu, L.; Moore, B.; Cucksey, C.; Risser, S. High Conductivity Transparent Carbon Nanotube Films Deposited from Superacid. *Nanotechnology* **2011**, *22*, 075201.
25. Saha, A.; Ghosh, S.; Behabtu, N.; Pasquali, M.; Martí, A. A. Single-Walled Carbon Nanotubes Shell Decorating Porous Silicate Materials: A General Platform for Studying the Interaction of Carbon Nanotubes with Photoactive Molecules. *Chem. Sci.* **2011**, *2*, 1682–1687.
26. Ramesh, S.; Ericson, L. M.; Davis, V. A.; Saini, R. K.; Kittrell, C.; Pasquali, M.; Billups, W. E.; Adams, W. W.; Hauge, R. H.; Smalley, R. E. Dissolution of Pristine Single Walled Carbon Nanotubes in Superacids by Direct Protonation. *J. Phys. Chem. B* **2004**, *108*, 8794–8798.
27. Parra-Vasquez, A. N. G.; Behabtu, N.; Green, M. J.; Pint, C. L.; Young, C. C.; Schmidt, J.; Kesselman, E.; Goyal, A.; Ajayan, P. M.; Cohen, Y.; *et al.* Spontaneous Dissolution of Ultralong Single- and Multiwalled Carbon Nanotubes. *ACS Nano* **2010**, *4*, 3969–3978.
28. Lefebvre, J.; Fraser, J. M.; Finnie, P.; Homma, Y. Photoluminescence from an Individual Single-Walled Carbon Nanotube. *Phys. Rev. B* **2004**, *69*, 075403.
29. Casey, J. P.; Bachilo, S. M.; Moran, C. H.; Weisman, R. B. Chirality-Resolved Length Analysis of Single-Walled Carbon Nanotube Samples through Shear-Aligned Photoluminescence Anisotropy. *ACS Nano* **2008**, *2*, 1738–1746.
30. Tsyboulski, D. A.; Bachilo, S. M.; Weisman, R. B. Versatile Visualization of Individual Single-Walled Carbon Nanotubes with Near-Infrared Fluorescence Microscopy. *Nano Lett.* **2005**, *5*, 975–979.
31. Carlson, L. J.; Krauss, T. D. Photophysics of Individual Single-Walled Carbon Nanotubes. *Acc. Chem. Res.* **2008**, *41*, 235–243.
32. Lefebvre, J.; Fraser, J. M.; Finnie, P.; Homma, Y. Photoluminescence from an Individual Single-Walled Carbon Nanotube. *Phys. Rev. B* **2004**, *69*, 75403.
33. Inoue, T.; Matsuda, K.; Murakami, Y.; Maruyama, S.; Kanemitsu, Y. Diameter Dependence of Exciton-Phonon Interaction in Individual Single-Walled Carbon Nanotubes Studied by Microphotoluminescence Spectroscopy. *Phys. Rev. B* **2006**, *73*, 233401.
34. Kiowski, O.; Jester, S. S.; Lebedkin, S.; Jin, Z.; Li, Y.; Kappes, M. M. Photoluminescence Spectral Imaging of Ultralong Single-Walled Carbon Nanotubes: Micromanipulation-Induced Strain, Rupture, and Determination of Handedness. *Phys. Rev. B* **2009**, *80*, 75426.
35. Dukovic, G.; White, B. E.; Zhou, Z.; Wang, F.; Jockusch, S.; Steigerwald, M. L.; Heinz, T. F.; Friesner, R. A.; Turro, N. J.; Brus, L. E. Reversible Surface Oxidation and Efficient Luminescence Quenching in Semiconductor Single-Wall Carbon Nanotubes. *J. Am. Chem. Soc.* **2004**, *126*, 15269–15276.
36. Jaques, D.; Leisten, J. A. 514. Acid-Catalysed Ether Fission. Part II. Diethyl Ether in Aqueous Acids. *J. Chem. Soc.* **1964**, 2683–2689.
37. Hecht, D. S.; Hu, L. B.; Irvin, G. Emerging Transparent Electrodes Based on Thin Films of Carbon Nanotubes, Graphene, and Metallic Nanostructures. *Adv. Mater.* **2011**, *23*, 1482–1513.

38. Shin, D.-W.; Lee, J. H.; Kim, Y.-H.; Yu, S. M.; Park, S.-Y.; Yoo, J.-B. A Role of HNO_3 on Transparent Conducting Film with Single-Walled Carbon Nanotubes. *Nanotechnology* **2009**, *20*, 475703.
39. Li, Z. R.; Kandel, H. R.; Dervishi, E.; Saini, V.; Xu, Y.; Biris, A. R.; Lupu, D.; Salamo, G. J.; Biris, A. S. Comparative Study on Different Carbon Nanotube Materials in Terms of Transparent Conductive Coatings. *Langmuir* **2008**, *24*, 2655–2662.
40. Lucas, A.; Zakri, C.; Maugey, M.; Pasquali, M.; van der Schoot, P.; Poulin, P. Kinetics of Nanotube and Microfiber Scission under Sonication. *J. Phys. Chem. C* **2009**, *113*, 20599–20605.
41. Hecht, D.; Hu, L.; Gruner, G. Conductivity Scaling with Bundle Length and Diameter in Single Walled Carbon Nanotube Networks. *Appl. Phys. Lett.* **2006**, *89*, 133112.
42. Graupner, R.; Abraham, J.; Vencelova, A.; Seyller, T.; Hennrich, F.; Kappes, M. M.; Hirsch, A.; Ley, L. Doping of Single-Walled Carbon Nanotube Bundles by Bronsted Acids. *Phys. Chem. Chem. Phys.* **2003**, *5*, 5472–5476.
43. Moulder, W. F. S.; Sobol, P. E.; Bomben, K. D. *Handbook of X-ray Photoelectron Spectroscopy*; Physical electronics, Inc.: Eden Prairie, Minnesota, 1995.
44. Sreekumar, T. V.; Liu, T.; Kumar, S.; Ericson, L. M.; Hauge, R. H.; Smalley, R. E. Single-Wall Carbon Nanotube Films. *Chem. Mater.* **2002**, *15*, 175–178.
45. Heller, D. A.; Barone, P. W.; Swanson, J. P.; Mayrhofer, R. M.; Strano, M. S. Using Raman Spectroscopy to Elucidate the Aggregation State of Single-Walled Carbon Nanotubes. *J. Phys. Chem. B* **2004**, *108*, 6905–6909.
46. Doorn, S. K.; Strano, M. S.; O'Connell, M. J.; Haroz, E. H.; Rialon, K. L.; Hauge, R. H.; Smalley, R. E. Capillary Electrophoresis Separations of Bundled and Individual Carbon Nanotubes. *J. Phys. Chem. B* **2003**, *107*, 6063–6069.
47. Chiang, I. W.; Brinson, B. E.; Huang, A. Y.; Willis, P. A.; Bronikowski, M. J.; Margrave, J. L.; Smalley, R. E.; Hauge, R. H. Purification and Characterization of Single-Wall Carbon Nanotubes (SWNTs) Obtained from the Gas-Phase Decomposition of CO (HiPco Process). *J. Phys. Chem. B* **2001**, *105*, 8297–8301.